Proceedings of the ASME 2013 Summer Heat Transfer Conference
HT2013
July 14-19, 2013, Minneapolis, MN, USA

HT2013-17001

MOLECULAR SIMULATION ON EXPLOSIVE BOILING OF WATER ON A HOT COPPER PLATE

Yijin Mao and Yuwen Zhang
Department of Mechanical and Aerospace Engineering
University of Missouri
Columbia, Missouri, 65211
Email: zhangyu@missouri.edu

ABSTRACT

In this paper, molecular dynamics simulation is carried out to study the explosive boiling of liquid water film heated by a hot copper plate in a confined space. A more physically-sound thermostat is applied to control the temperature of the metal plate and then to heat water molecules that are placed in the elastic wall confined simulation domain. The results show that liquid water molecules close to the plate are instantly overheated and undergo an explosive phase transition. A huge pressure in the region between liquid film and hot copper plate formed at the beginning and leads to a low density vapor region by partially vaporizing water film. A non-vaporization molecular layer, with a constant density of 0.2 g/cm^3, tightly attached to the surface of the plate is observed. The z-component of COM (center of mass) trajectory of the liquid film in the confined space is tracked and analyzed. The one-dimensional density profile indicates the water film have a piston-like motion after short period of explosive boiling. Temperatures at three corresponding regions, which are vapor, liquid, and vapor from the top plate surface, are also computed and analyzed along with the piston-like motion of the bulk liquid film.

INTRODUCTION

Explosive boiling can find its applications in various industrial fields, including laser cleaning, thermal ink-jet printer, medical surgery, and so on[1-3]. Different from normal boiling which allow heterogeneous bubble nucleation of the vapor bubble, the liquid is superheated to a degree much higher than the normal saturation temperature and approaching the thermodynamic critical temperature; homogeneous vapor bubble nucleation takes place at an extremely high rate, which lead to the near-surface region of the materials being ejected explosively [4], and waves could be created on the liquid surface during the explosive boiling. The explosive boiling is also referred to as vapor explosion, phase flashing, thermal detonation, and rapid phase transitions. Many special events occur during explosive boiling, such as pressure shock wave, bubble clusters formed by tiny bubbles, and high superheat. Many experimental works are reported [5-11], but these experimental works are limited in either length or time scales. In addition, because of the limitation of classical macroscopic theory, many special phenomena in phase explosion cannot be well explained.

A molecular dynamics (MD) simulation, which has advantages of describing any physical process at atomic level, is widely applied to study micro- and nanoscale heat and mass transfer problems. Dou et al. presented a microscopic description on explosive boiling of water films adjacent to heated gold surface, and found that the vaporization phenomena highly depended on the initial thickness of the water film [12]. Thinner films fragmented completely and dissolved into a mixture of small cluster and water molecules, while only the near-surface water layers vaporized for the thicker film. Gu and Urbassek performed MD simulation on explosive boiling of liquid-argon films irradiated by ultrafast laser [13]. It was also found that liquid argon would completely fragment if the thickness was below seven monolayers, while for thicker film only the near-surface argon layers vaporized. Zou and Huai studied the bubble nucleation rate in a confined water film between two metal plates, and it was found that the nucleation rate was 10 orders of magnitude higher than that predicted by the classical theory, and was 1 order of magnitude higher than that measured by the experiment of explosive boiling [14]. The same group also simulated a homogenous nucleation of water and liquid nitrogen in the explosive boiling, and energy conversion and redistribution were studied [15].

Though the existing MD work have provided some molecular level understandings of the phase transition in the explosive boiling, fewer work revealed the thermal and

dynamic mechanisms caused by an extremely high heat flux through metal plate, like copper. Moreover, few researchers paid attentions on the dynamic phenomenon associated with different phases after the explosive boiling, although mechanical factor (like thermal stress) was always considered as an important effect determining machining performance in most applications. In this paper, both thermal and dynamic phenomena of a thick water film will be investigated during and after explosive boiling.

PHYSICAL MODELS AND METHODS

The computational domain is divided into three regions, namely vapor, liquid and solid region. Both vapor and liquid regions are filled with water molecules, and the solid is a copper plate. In consideration of accuracy in description of water's dynamic and thermal properties, a four-site water model (TIP4P) [16] is adapted to model vapor and liquid water. The well-accepted Lennard Jones-like potential potential, which consists of the contributions from electrostatic, dispersion and repulsive forces, is used to describe intermolecular interaction of water molecules:

$$U_{ab} = \sum_{i}^{a}\sum_{j}^{b} \frac{k_C q_{a_i} q_{b_j}}{r_{a_i b_j}} + \sum_{i}^{a}\sum_{j}^{b} 4\varepsilon_{a_i b_j}\left[\left(\frac{\sigma_{a_i b_j}}{r_{a_i b_j}}\right)^{12} - \left(\frac{\sigma_{a_i b_j}}{r_{a_i b_j}}\right)^{6}\right] \quad (1)$$

where, *a* and *b* denote two different molecules, subscript *i* and *j* represent atoms of hydrogen or oxygen in one individual TIP4P molecule, and k_c is the electrostatic constant. The long-range columbic contribution to the entire system is computed by PPPM approach [17] with accuracy of 1.0×10^{-6}. It should be pointed out that the pair potential only counts the interaction between oxygen atoms within the cutoff distance of 12 Å; both bond and angle interactions within a single water molecule are considered as harmonic. In addition, SHAKE [18] algorithm is applied to each water molecule to hold its geometry shape such that a longer time step of 1 fs can be utilized. The water region is built with face-center cubic unit (FCC) with lattice constant of 37.0 Å and 3.103 Å, respectively, subject to the densities of vapor and liquid at 1 atm [19]. For the copper plate, it is also modeled with face-centered cubic unit (FCC) with the lattice constant of 3.615 Å, which is consistent with the density of 8.9×10^3 kg/m^3. It should be mentioned that the interaction between copper atoms are not considered, instead, many artificial Cu-Cu harmonic bonds are created for the plate to introduce Cu-Cu spring-like interaction, which will be discussed later. The interaction between copper and oxygen or hydrogen atoms are considered using the Lenard Jones potential.

In order to introduce a more physically-sound thermostat to create heat flux through copper plate rather than artificially rescaling velocity of atoms, the copper plate is modeled using the approach described in [20]. As shown in Fig. 1, five layers of atoms are created in FCC configuration. The top three layers (white) are "real" copper atoms. The fourth layer (blue) is considered to be phantom atoms exerted with a force combined with a damping force and random force that subject to Gaussian distribution. The fifth layer is fixed in order to prevent atoms from penetration. The standard deviation of the random force is,

$$\sigma_F = \sqrt{\frac{2\alpha k_B T}{\Delta t}} \quad (2)$$

where α is dependent on desired temperature and integration time length,

$$\alpha = \frac{m\omega_D \pi}{6} \quad (3)$$

where Debye frequency ω_D can be estimated by,

$$\omega_D = \left(\frac{3}{4\pi}\frac{N}{V}\right)^{\frac{1}{3}} v_s \quad (4)$$

where v_s is the speed of sound in the solid. Thus, the energy flux to the simulation system can be accurately calculated by integrating the exciting force and the damping force applied to those phantom atoms. It can also be seen from Fig. 1 that an artificial harmonic bond is created by connecting neighbor copper atoms that are within its shortest distance of 2.56 Å.

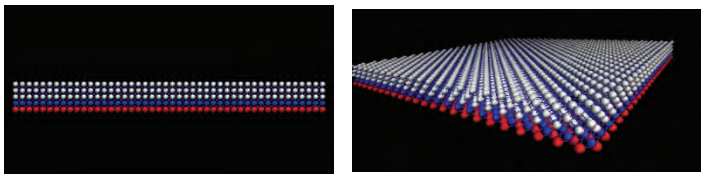

(a) front view (b) perspective view

Figure 1 Structures of the copper plate, artificial harmonic bond are created by connecting neighbor atom within a distance of 2.56 Å.

Since the interaction between atoms within the second layer of phantom atom is modeled with artificial harmonic bond, it is important to use a reasonable spring constant to obtain an accurate thermostat. The interatomic spring constant *k* is tightly related to Young's Modules thus it could be estimated with formula below,

$$k = Ed \quad (5)$$

where *E* is Young's Modules of solid copper, and *d* is corresponding lattice constant of solid metal. Table 1 gives all the parameters required in this simulation.

Table 1 water potential parameters

Parameters	Values	Units
ε_{OO}	0.006998	eV
σ_{OO}	3.16438	Å
q_{H}	0.52	e
q_{O}	-1.04	e
ε_{CuO}	0.06387	eV
σ_{CuO}	2.7172	Å
ε_{CuH}	0.03396	eV
σ_{CuH}	1.335	Å
E	274~306	GPa
d	3.615	Å
vs	3901	m/s

The simulation is carried out within the framework of the open Source MD code LAMMPS [21]. The entire simulation box has both length and width of 82.89 Å, and a height of 240 Å. Periodic boundary conditions are applied to all directions parallel to the surface of the plate, while an elastic wall is placed at the top to seal the simulation box. The water regions are filled with 12,504 molecules (~6.2 nm in thickness) and there are 5,290 copper atoms in the hot plate. Before the liquid water is heated by the hot plate, the system must be equilibrated in the following two steps: (1) the entire water zones are first equilibrated with Berendsen thermostat [22] until the temperature of water system was equilibrated to a stable value of 298 K, and (2) the copper plate is then heated to 1000 K with "phantom atom" thermostat as stated above while the water molecules are isolated from the integration. After those preparations steps are done, the liquid water at 298 K is suddenly placed on the hot plate. The entire system is still integrated with NVE ensemble during the simulation and copper plate is still controlled to desired temperature of 1000K with "phantom atom" thermostat. The value of 1000K is chosen to guarantee that the temperature above the threshold as above in bubble formation [23] while it is still below the melting point of copper.

RESULTS AND DISCUSSIONS

The monitored temperatures of the copper plate and entire water region are recorded and shown in Fig. 2. It can be seen that there is an obvious temperature drop from 1000 K to a minimum value of 800 K when the "cold" water film touches the hot plate due to heat conduction mechanism of solid copper. It takes around 50 ps before the temperature of the hot copper turning back to 1000 K because of the continuingly added heat flux. The temperature of water region keeps increasing from 298 K to 400 K during the initial 80 ps.

Figure 3 gives several snapshots of molecules spatial distribution at representative times (the arrow in the parenthesis denotes the moving direction of the bulk fluid). An obvious volume expansion of liquid water can be observed during the period from 10 to 20 ps by measuring the height of the liquid film. A low density vapor region appears at time of 30 ps, and the entire water domain can be clearly divided into three

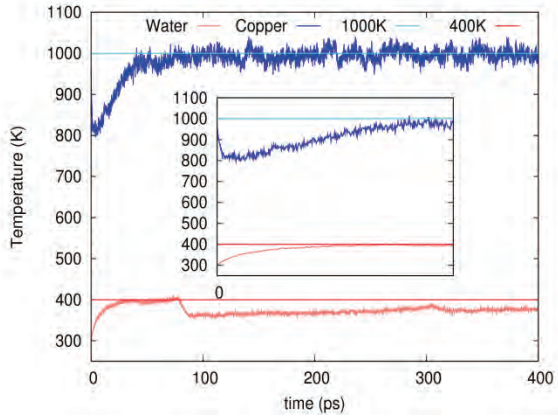

Figure 2 Temperature variations of water and hot copper plate

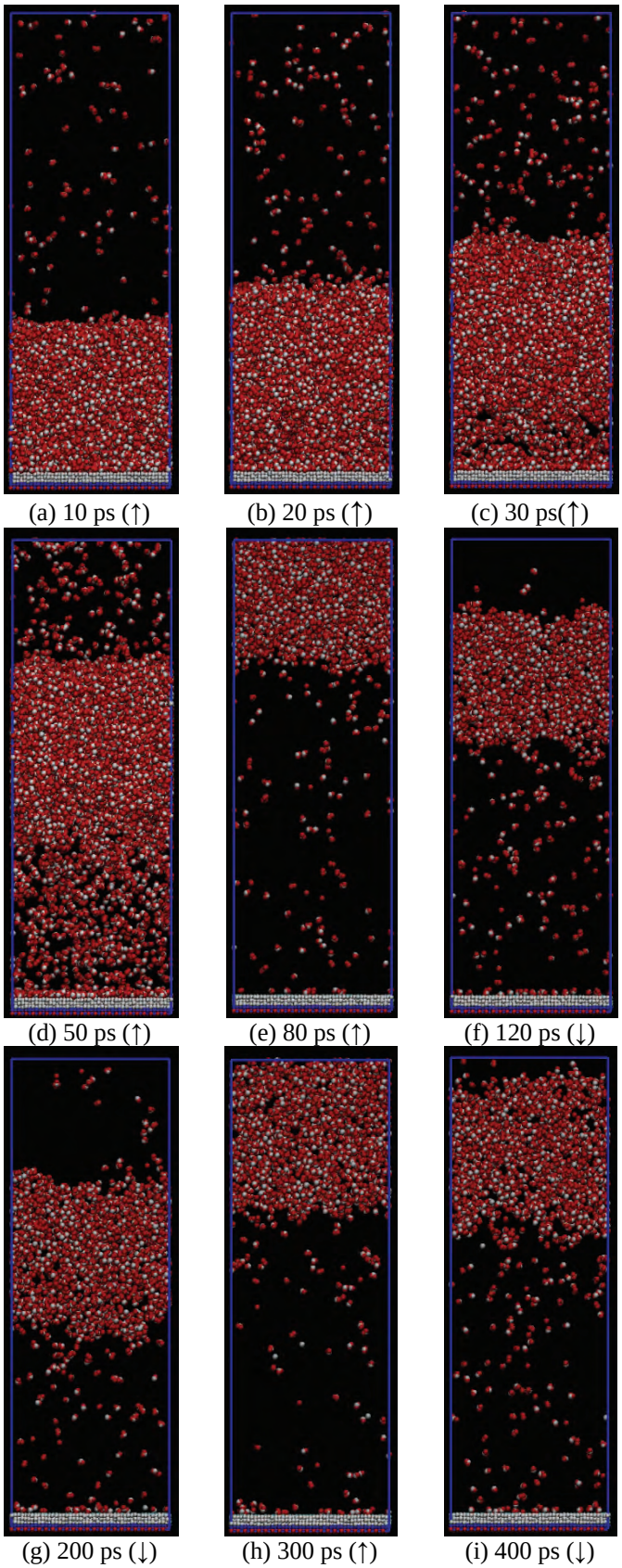

Figure 3 Water molecule distribution for time 10 to 400 ps.

regions: top vapor region, liquid region and the lower vapor region near the hot plate. Due to continuous heat flux absorbed by water molecules, the lower vapor region keeps expanding up to 80 ps when the water film collide with the top wall. During this period, the entire wall surface is covered by vapor and the water film floats on the top of the vaporized water molecules layer in a manner reminiscent of the Leidenfrost phenomenon [24].

After the elastic collision with the wall, the film is forced to move backward, as shown in Fig. 3(f). At approximately 200 ps, water film starts moving upward again due to larger pressure in the lower vapor region. The film hits against the top wall and rebound at 300 ps and suspended at 400 ps again. In corresponding to piston-like motion of liquid film, the COM's trajectory (*z*-component) of water region is recorded and shown in Fig. 4. The period from 0 to 80 ps is explosive boiling transition, and the rest is the bulk liquid's piston-like motion moment. It can be seen that the stationary point is flatter and higher, which means that the bulk liquid water will be stationary and eventually suspended somewhere adjacent to the wall due to the fact that the system keeps receiving the constant flux through copper plate.

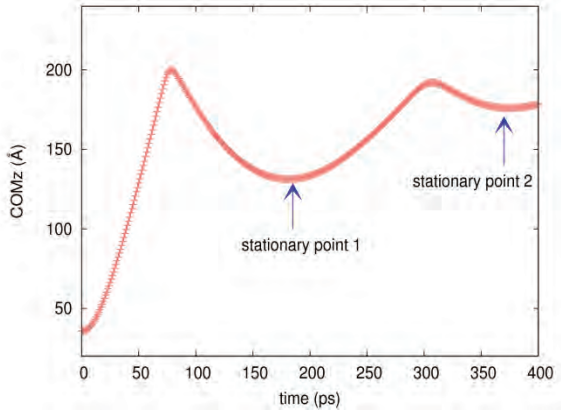

Figure 4 z-component of COM associated to water molecules within the simulation box

In order to have a closer look at the density variation, the spatial density profile is computed by averaging density in 63 bins which are built by uniformly chopping the simulation box in the vertical direction; the final profile of density are shown in Fig. 5 and the bulk liquid water moving directions are denoted by the arrow. It can be seen that the maximum bulk liquid density keeps decreasing during the moving process until it impact with the wall (see Fig. 5(a)) due to explosive boiling. The increasing of the maximum density at 80 ps comes from the water molecules' compression due to their inertia when they hits against the wall. In Fig. 5(b), the maximum density also decreases when the bulk liquid moving backward mainly due to liquid expansion. Comparison between Figs. 5 (c) and (d) indicates that the maximum density does not change anymore and the height of the bulk liquid water keeps almost a constant; this indicates that phase change at the liquid-vapor interface is balanced during this period. Interestingly, a non-vaporized water molecule layer always exists at the interface between solid copper and lower vapor region no matter how long the heating processing lasts. This special zone, which is denoted as "hot gas-like zone", is also observed during evaporation process [25]. The density of this zone decreases during the period of explosive boiling and gradually stabilized at 0.2 g/cm^3. Figure 6 shows the variation of the "hot gas-like" water molecule distribution on the surface of the copper plate. From 0 to 60 ps, it can be seen more and more localized "dry" region appears on the wall surface. However, during the later period, a fixed number of hot gas-like water molecules attached on the copper plate even continuous heat flux flows through the plate to water regions.

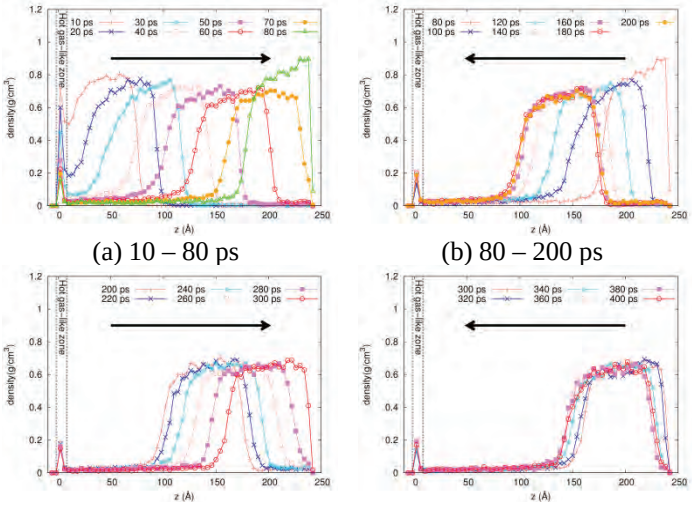

(a) 10 – 80 ps (b) 80 – 200 ps

(c) 200 – 300 ps (d) 300 – 400 ps

Figure 5 One-dimensional spatial density distribution at various times.

The temporal density profile is also computed and rendered into a 2-D plot in Fig. 7 where the vertical axis is the distance measured from the surface of the copper plate and the horizontal axis is the simulation time. The band that represents the bulk water film becomes narrower and narrower during the period of explosive boiling (0-80ps). It expands a little back to original thickness and keeps constant due to phase transition balance at the interface, which is consistent with the results in Fig 5.

The temporal variation of one dimensional temperature distribution in the vertical direction is shown in Fig. 8. It can be seen that the temperature variation in time and space are extremely large though the bulk temperature of the water are relatively stable as shown in Fig. 2. The maximum temperature is 1593 K while the minimum is around 300 K. It should be noticed that 0 K in the legend of Fig. 8 is the temperature at lower layer of copper plate which is fixed as stated previously. However, the spatial variation is smaller along the time axis as the color gradient, especially at the liquid-vapor interface, is smoother and smoother in Fig 8. A similar band to Fig. 7 can also been seen in this figure if take a close look. As a result of "colder" molecules in the top vapor region due to compression, a temperature fall appears during time period from 80 to 300 ps, which occurs after the first rebound of water film.

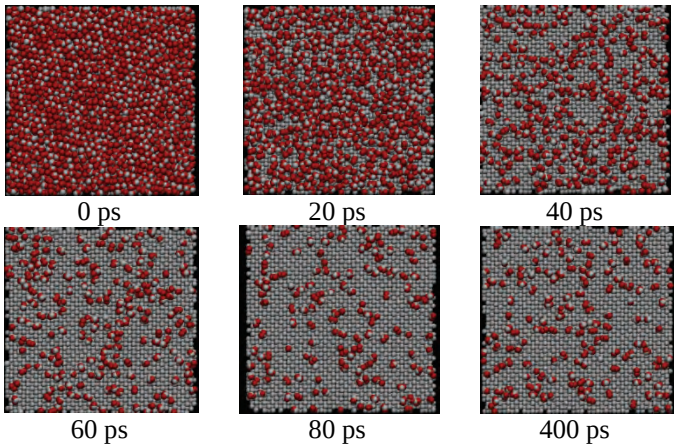

Figure 6 Top views of water molecules distribution on the surface of the copper plate

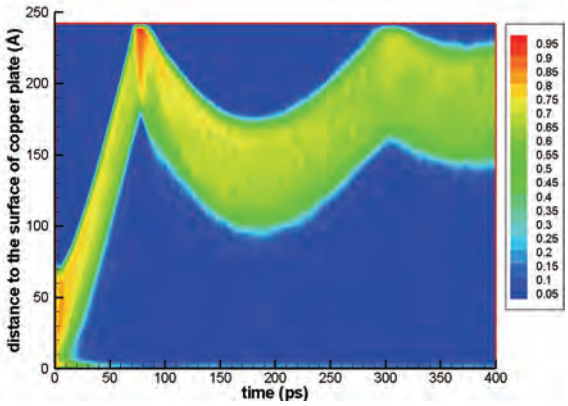

Figure 7 Variation of one dimensional spatial density distribution with time.

As shown in the previous snapshots, there are three regions appearing during the simulation. According to the one-dimensional density distribution, they can be easily found by locating the liquid-vapor interface as the following steps: (1) obtaining the one-dimensional density distribution by uniformly chopping the water region into n pieces, and (2) filtering the density profile by a sawtooth window function which has a height of water critical density and has a width of p points ($p \geq 2$). Two scenarios can be considered as phase interface: one is when the average value of the former $p/2$ points is lower than critical density and the value of latter $p/2$ points is higher; the other is that if the average value of the former $p/2$ is higher than critical density and the that of the latter is lower. The width p should be appropriately chosen to achieve a reasonable resolution of detecting the density jump at the phase transition zone. In this case, the p value is 3, n is 63, and critical density of water is 0.32g/cm^3 [19].

Figure 9 shows the temperature variation in each region by dynamically detecting the liquid-vapor interfaces. During the period of explosive boiling, temperature in the lower vapor region is much higher than middle liquid film and top vapor regions. The maximum temperature of lower vapor region is 780 K which is only 220 K below the initial temperature of the plate (1000 K). In consideration of the temperature drop of the plate, the temperature difference between bottom vapor and copper plate is even smaller. For the lower vapor region, it can be seen that temperature suddenly fell at around 45 ps when the vapor regions is fully expanded such that the amount of kinetic energy of molecules are converted to potential energy.

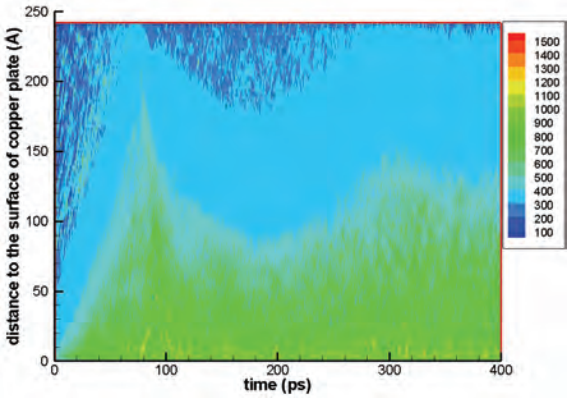

Figure 8 Variation of one dimensional spatial temperature distribution with time.

A similar drop also appear in middle bulk water film due to energy conversion to potential energy during mass flux flow to the lower vapor region. For the newly created vapor region, an increase at time 70 ps is caused by absorbing the heat flux continuously entering the vapor region. Because the compression process where the kinetic energy is converted to be potential energy again when bulk liquid hit against the wall, a temperature drop occurs again. Since all the three regions are compressed at this time, so all of them have a drop at 80 ps. Similarly, at 300 ps, an obvious temperature drop appeared in middle bulk liquid and top vapor again due to compression. The temperature in the lower vapor region does not fall because the volume of this region is larger enough to overcome the kinetic energy loss due to compression. In addition, continuously entering heat flux provides enough energy to fill the small amount of the lost energy.

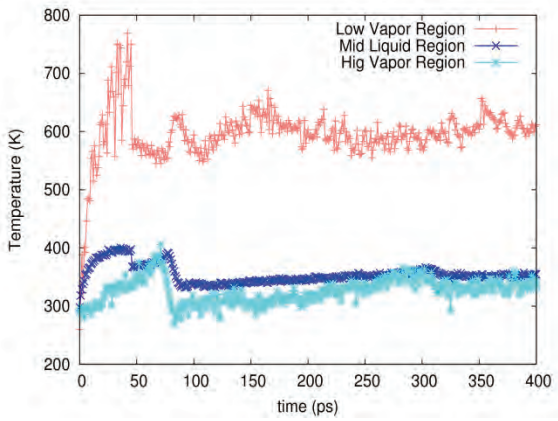

Figure 9 Temperature variations in three regions.

CONCLUSIONS

Molecular dynamics simulation is carried out to study the explosive boiling of liquid water film on a hot copper plate. It is found that the hot plate is first cool down by the "cold water" when the liquid film touches it. But the copper plate temperature gradually turns back to 1000 K within the ~50 ps. In comparison, the bulk temperature of water molecules keeps increasing up to 400 K during the period before the film hits the wall by continuously absorbing the entering energy. After phase explosion, the bulk liquid water moves like a piston with two vapor regions at bottom and top. It is observed that a temperature drop occurs when the bulk liquid film impact with the top wall due to energy conversion between kinetic and potential energy for water molecules. The trajectory variation of water molecule's COM value (*z*-component) indicates that the piston-like motion of the liquid film will finally stop and suspended somewhere close to the top wall. A group of non-vaporization molecular, which has a constant density of 0.2 g/cm^3 and tightly attached to the localized "dry" surface of the plate, is observed no matter how long the heat process lasts. It is also found that temperature at each region decreases during the compression process where kinetic energy of molecules is converted to potential energy when water film hits the fixed top wall.

ACKNOWLEDGMENTS

Support for this work by the U.S. National Science Foundation under grant number CBET- 1066917 is gratefully acknowledged.

REFERENCES

[1] Morimoto, A, Tanimura, H., Yang, H., Otsubo, S., Kumeda, M., Chen, X., Platimum Film Patterning by Laser Lift-off using Hydrocarbon Film on Insulating Substrates, Applied Physics A, 2004, 79, 1015-1018.

[2] Lang, F., Mosbacher, M., Leiderer, P., Applied Physics A: Materials Science Process, Near field induced defects and influence of the liquid layer thickness in Steam Laser Cleaning of silicon wafers, 2003, 77, 117-123.

[3] Kudryashov, S. I., and Allen, S. D., Viscous drag force effect on transportation of submicron particle contaminants during dry and steam laser cleaning, Proc. SPIE 5713: Photon Processing in Microelectronics and Photonics IV, 528, 2005, doi: 10.1117/12.587101.

[4] Faghri, A., and Zhang, Y., Transport Phenomena in Multiphase Systems, 2010, Elsevier, Burlington, MA.

[5] Kudryashov, S. I., Lyon, K., Allen, S. D., Laser-Induced Cavitation and Explosive Boiling in Superheated Liquids: a New GHz Probe. Phipps C R. High-Power Laser Ablation VI, New Mexico: American Institute of Physics, 2006, 1- 10.

[6] Kudryashov, S., and Allen, S. D., Experimental and Theoretical Studies of Laser Cleaning Mechanisms for Submicrometer Particulates on Si Surfaces, Particulate Science and Technology, 2006, 24(3), 281-299.

[7] Xu, X. F., Phase Explosion and Its Time Lag in Nanosecond Laser Ablation, Applied Surface Science, 2002, 197, 61-66.

[8] Kudryashov, S. I., and Allen, S. D., Submicrosecond Dynamics of Water Explosive Boiling and Lift-off from Laser-heated Silicon Surfaces, Journal of Applied Physics, 2006, 100, 104908.

[9] Yin, T. N., and Huai, X. L., Fourier and Wavelet Transform Analysis of Pressure Signals during Explosive Boiling, Chinese Physics Letter, 2008, 25(3), 1004-1007.

[10] She, M., Kim, D., and Grigoropoulos, C. P., Liquid-assisted Pulsed Laser Cleaning using Near-infrared and Ultraviolet Radiation, Journal of Applied Physics, 1999, 86(11), 6519-6524.

[11] Takamizawa, A., Kajimoto, S., Hobley, J., Hatanaka, K., Ohta, K., and Fukumura, H., Explosive Boiling of Water after pulsed IR Laser Heating, Physical Chemistry Chemical Physics, 2003, 5, 888-895.

[12] Dou, Y. S., Zhigilei, L. V., Winograd, N., and Garrison, B., Explosive Boiling of Water Films Adjacent to Heated Surfaces: A Microscopic Description, Journal of Physical Chemistry, 2001, 105, 2748-2755.

[13] Gu, X., and Urbassek, H. M., Atomic Dynamics of Explosive Boiling of Liquid-Argon Films, Applied Physics B, 2005, 81, 675-679.

[14] Zou, Y., and Huai, X. L., A Molecular Dynamics Simulation of Bubble Nucleation on Solid Surface in Explosive Boiling, ASME 2009 International Mechanical Engineering Congress & Exposition, Lake Buena Vista, Florida, 1727-1733.

[15] Zou, Y., Huai, X. L., and Lin, L., Molecular Dynamics Simulation for Homogeneous Nucleation of Water and Liquid Nitrogen in Explosive Boiling, Applied Thermal Engineering, 2010, 30, 859-863.

[16] Jorgensen, W. L., Chandrasekhar, J., and Madura, J. D., Comparison of Simple Potential Functions for Simulating Liquid Water, Journal of Chemical Physics, 1983, **79**,. 926-935.

[17] Hockney, R. W., Eastwood, J. W., Computer Simulation Using Particles, 1st ed., 1998, Taylor & Francis, New York, NY.

[18] Ryckaert, J. P., Ciccotti, G., and Berendsen, H. J. C., Numerical Integration of the Cartesian Equation of Motion of a System with Constraints: Molecular Dynamics of n-Alkanes, Journal of Computational Physics, 1997, 23, 327-341.

[19] Haynes, W. M., *Handbook of Chemistry and Physics*, 91st ed., Taylor & Francis, New York, NY, Chap. 6.

[20] Yi, P., Poulikakos, D., Walther, J., and Yadigaroglu, G., Molecular Dynamics Simulation of Vaporization of an Ultra-thin Liquid Argon Layer on a Surface, International Journal of Heat and Mass Transfer, 2002, 45, 2087-2100.

[21] Plimpton, S. J., 1995, Fast Parallel Algorithms for Short-Range Molecular Dynamics, Journal of Computation Physics, 117, pp. 1-19.

[22] Hünenberger, P. H., 2005, Thermostat Algorithms for Molecular Dynamics Simulations, Advance in Polymer Science, 173, pp. 105-149.

[23] Lin, C. P., and Kelly, M. W., Cavitation and Acoustic Emission around Laser-heated Microparticles, Applied Physics Letters, 1998, 72 (22), 2800-2802.

[24] Garmett, W. M., Leidenfrost's Phenomenon, Nature, 1878, 466-466.

[25] Yu, J. P., and Wang, H., A Molecular Dynamics Investigation on Evaporation of Thin Liquid Films, International Journal of Heat and Mass Transfer, 2012, 55, 1218-1225.